PHYSICAL REVIEW B **84**, 054513 (2011)

Electrochemical synthesis and superconducting phase diagram of $Cu_xBi_2Se_3$

M. Kriener,[1,*] Kouji Segawa,[1] Zhi Ren,[1] Satoshi Sasaki,[1] Shohei Wada,[1] Susumu Kuwabata,[2] and Yoichi Ando[1,†]

[1]*Institute of Scientific and Industrial Research, Osaka University, Osaka 567-0047, Japan*

[2]*Department of Applied Chemistry, Osaka University, Osaka 565-0871, Japan*

(Received 6 June 2011; revised manuscript received 12 July 2011; published 8 August 2011)

The superconducting $Cu_xBi_2Se_3$ is an electron-doped topological insulator and is a prime candidate of the topological superconductor which still awaits discovery. The electrochemical intercalation technique for synthesizing $Cu_xBi_2Se_3$ offers good control of restricting Cu into the van der Waals gap and yields samples with shielding fractions of up to ∼50%. We report essential details of this synthesis technique and present the established superconducting phase diagram of T_c vs x, along with a diagram of the shielding fraction vs x. Intriguingly, those diagrams suggest that there is a tendency to spontaneously form small islands of optimum superconductor in this material.

DOI: 10.1103/PhysRevB.84.054513 PACS number(s): 74.25.Dw, 74.62.−c, 82.45.Vp, 65.40.gk

I. INTRODUCTION

Topological insulators (TIs) are attracting great interest since they realize a new state of matter; namely, the bulk of such materials is insulating, but in contrast to conventional band insulators, their bulk wave functions exhibit a nontrivial Z_2 topology leading to gapless and hence conductive surface states.[1–3] Those topological surface states are interesting because they exhibit a Dirac-like energy dispersion (similar to that in graphene) and a helical spin polarization, both of which hold promise for various energy-saving device applications.[4–6] Soon after the theoretical predictions of candidate materials,[7,8] a series of promising materials were experimentally discovered to be three-dimensional (3D) TIs,[9–21] stimulating the search for a superconducting analog, i.e., a topological superconductor, which is characterized by a full energy gap in the bulk and the existence of gapless surface Andreev bound states.[22–27] Such a topological superconductor is predicted to be a key to realizing a fault-tolerant topological quantum computing,[22] and the discovery of a concrete example of the topological superconductor would have a large impact on future technology. In this context, there is an intriguing prediction that when superconductivity is achieved by doping a topological insulator, it may realize a topological superconducting state.[28]

Recently, Hor *et al.*[29] reported superconductivity in the electron-doped TI material $Cu_xBi_2Se_3$ for $0.1 \leqslant x \leqslant 0.3$, where the layered TI compound Bi_2Se_3 was intercalated with Cu. Their samples showed superconductivity below critical temperatures $T_c \leqslant 3.8$ K. In a subsequent study on these samples,[30] it was further found that the topological surface states remain intact upon Cu intercalation. Thus, $Cu_xBi_2Se_3$ is the first promising candidate material to be a topological superconductor, and it is very important to elucidate the nature of its superconducting state. However, the samples prepared by Hor *et al.* showed superconducting shielding fractions of only less than 20% and the resistivity never really disappeared below T_c.[29,30] Therefore, some doubts remained about the bulk nature of the superconducting phase in $Cu_xBi_2Se_3$, and preparations of higher quality samples were strongly called for.

In our recent experiments,[31] we succeeded in synthesizing $Cu_xBi_2Se_3$ samples with shielding fractions of up to 50% (depending on the Cu concentration) by applying a different sample preparation method than the standard melt-growth method employed in Ref. 29. In our high-quality samples, besides observing zero resistivity, we were able to measure the specific-heat anomaly in the superconducting phase, which indicated that the superconductivity in this material is a bulk feature and, moreover, appears to have a full energy gap,[31] which is a prerequisite to topological superconductivity.[23] In this paper, we describe in detail the newly applied preparation method of $Cu_xBi_2Se_3$ to employ electrochemical intercalation, and present the electronic phase diagram of T_c vs Cu concentration x. We also show how the superconducting shielding fraction of the electrochemically prepared samples changes with x, which bears an intriguing implication of intrinsically inhomogeneous superconductivity.

II. SAMPLE PREPARATIONS

Pristine Bi_2Se_3 has a layered crystal structure ($R\bar{3}m$, space group 166) consisting of stacked Se–Bi–Se–Bi–Se quintuple layers. The rhombohedral [111] direction is denoted as the c axis and the (111) plane as the ab plane. The neighboring quintuple layers are only weakly van der Waals bonded to each other. Cu is known to enter Bi_2Se_3 either as an intercalant in the van der Waals gaps or as a substitutional defect to replace Bi. In the former case, Cu^+ is formed and acts as a donor, whereas in the latter case, it creates two holes by replacing three Bi $6p$ electrons by one Cu $4s$ electron upon forming a σ bond. Therefore, Cu acts as an ambipolar dopant for Bi_2Se_3.[32,33] The melt-growth method employed by Hor *et al.*[29] cannot avoid the formation of substitutional Cu defects; in contrast, our electrochemical method has a distinct advantage to promote only the intercalation of Cu.

For the present experiments, we first grew single crystals of pristine Bi_2Se_3 by melting stoichiometric amounts of high-purity elemental shots of Bi (99.9999%) and Se (99.999%) at 850 °C for 96 h in sealed evacuated quartz glass tubes, followed by a slow cooling to 550 °C over 72 h and annealing at that temperature for 48 h. Before the electrochemical intercalation procedure, those melt-grown Bi_2Se_3 single crystals were cleaved and cut into rectangular pieces. They were wound by 50-μm thick, bare Cu wire and acted as the working electrode (WE). A 0.5-mm thick Cu stick was used both as the counter (CE) and reference electrode (RE) in our simplified setup sketched in Fig. 1(a).

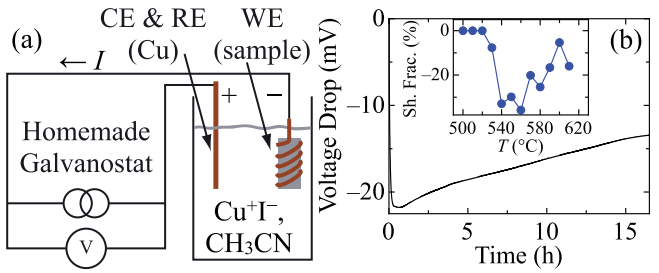

FIG. 1. (Color online) (a) Sketch of our simplified electrochemical intercalation setup. The counter electrode (CE) is also used as reference electrode (RE). The current direction is indicated. (b) Typical time dependence of the voltage drop measured between working and counter electrodes. The inset summarizes the development of the diamagnetism (plotted in terms of the shielding fraction) in a sample with $x = 0.31$ upon annealing at different temperatures.

Since Hor *et al.*[29] reported that $Cu_xBi_2Se_3$ samples are sensitive to air, the pristine Bi_2Se_3 samples were transferred into a glove box and the electrochemical intercalation of Cu was done in an inert atmosphere. To provide the electrical wiring required for electrochemical intercalation processes as sketched in Fig. 1(a), our glove box was specially modified for air-tight electrical connections. For the intercalation, we used a saturated solution of CuI powder (99.99%) in acetonitrile CH_3CN. A current of 10 μA was applied to the electrodes for a suitable time period to give the desired Cu concentration x. The typical time dependence of the voltage drop between the standard and working electrodes observed for our samples is shown in Fig. 1(b). Its absolute value was usually between -10 and -30 mV. The whole process was controlled by a computer which was also used to determine the total transferred charge.

After the intercalation had finished, the Cu concentration x in the sample was determined from its weight change: we measured the weight before and after the intercalation process with a high-precision balance with a resolution of 0.1 μg, and the possible error in x was less than ± 0.01. Note that this direct measurement of the Cu concentration is expected to be more accurate than most of the chemical analysis methods.[34] Nevertheless, we have also employed the inductively coupled plasma atomic-emission spectroscopy (ICP-AES) analysis, which is a destructive method but is good at giving absolute numbers, to confirm that the x values determined from the weight change is indeed reliable, as will be described later.

For a consistency check of our electrochemical intercalation process, we have calculated the total charge transferred during the intercalation. The experimentally determined Faraday number for our samples was usually up to 15% smaller than the theoretical Faraday constant, 96 485 C/mol. In this regard, it was reported[32,33] that a simple physical attachment of Cu metal to Bi_2Se_3 crystal results in a perceptible diffusion of Cu^+ into the van der Waals gaps of Bi_2Se_3. This reaction can be described as the following oxidation and reduction formulas in an electrochemical viewpoint:

$$x\mathrm{Cu} \rightarrow x\mathrm{Cu}^+ + xe^- \quad (1)$$

$$\mathrm{Bi_2Se_3} + xe^- \rightarrow (\mathrm{Bi_2Se_3})^{x-}. \quad (2)$$

The occurrence of electron transfer from Cu to Bi_2Se_3 implies that the redox potential of $Cu^{+/0}$ is more negative than that of $(Bi_2Se_3)^{0/x-}$. Since we are using a Cu wire to hold the sample and to make the electrical contact, it is possible that this wire became the source of an additional Cu^+ intercalation to the sample(s). This reaction should not be included into the charge balance, and hence the difference between the estimated and the theoretical Faraday numbers is naturally expected. This inference is supported by our observation that the sample mass increased even without applying a current, though at a much lower reaction rate.

It is most likely that the electrochemical intercalation is induced by reduction of Bi_2Se_3 without reduction of Cu^+, yielding $(Cu^+)_x(Bi_2Se_3)^{x-}$. This implies that doping of electrons with the nominal fraction of x should take place upon Cu^+ intercalation. The reaction at the counter electrode seems to be oxidation of Cu metal rather than that of I^- to I_2 or I_3^-, because the former redox potential is more negative than the latter one in an aqueous medium.

It is important to note that the as-intercalated samples *do not* superconduct yet. It turned out that the samples have to be annealed in order to establish superconductivity. For this purpose, the samples were sealed under vacuum in quartz glass tubes and put into a muffle furnace. For the determination of the optimum annealing temperature, one sample with $x = 0.31$ was annealed subsequently for 2 h at different temperatures starting at 500 °C. After each annealing run, the diamagnetic response was checked, and the result is shown in the inset of Fig. 1(b). A trace of diamagnetism indicating the appearance of a superconducting phase was detected after annealing at 530 °C, and the annealing temperature of 560 °C was found to yield the largest shielding fraction. When the sample was annealed at higher temperatures than 560 °C, the shielding fraction was found to be reduced irreversibly. (The onset T_c was essentially independent of the annealing temperature.) Therefore, the samples used for determining the phase diagram presented here were treated in the following way: they were heated up to 540 °C in 1 h, and then the temperature was gradually increased to 560 °C in 40 min to avoid any overheating; the samples were kept at 560 °C for 2 h and eventually quenched by dropping the quartz glass tubes into cold water.[35] We will come back later to the question of what is happening during the annealing process to activate the superconductivity.

To confirm the accuracy of the x values determined by the mass change (and also to make sure that the Cu content does not change appreciably during the annealing process), we measured the x values of eight of our samples in the post-annealed state by using the ICP-AES analysis (the sample mass was between 15 and 38 mg). For this destructive analysis, the whole sample was dissolved in nitric acid HNO_3. The Cu concentrations obtained from the ICP-AES analyses for the eight samples agreed with those obtained from the mass change within ± 0.014,[36] giving confidence in the x values reported in this paper.

In addition to the ICP-AES analysis, we have employed the electron-probe microanalyzer (EPMA) to check the distribution of Cu within the sample after the annealing. For this analysis, one sample with $x = 0.31$ was cleaved and subsequently scanned over distances of 10 μm and 1 mm, as sketched in Fig. 2(c). The intensity of the characteristic x-ray of each element is plotted vs the scan position for the two different scan lengths in Figs. 2(a) and 2(b). One can see that

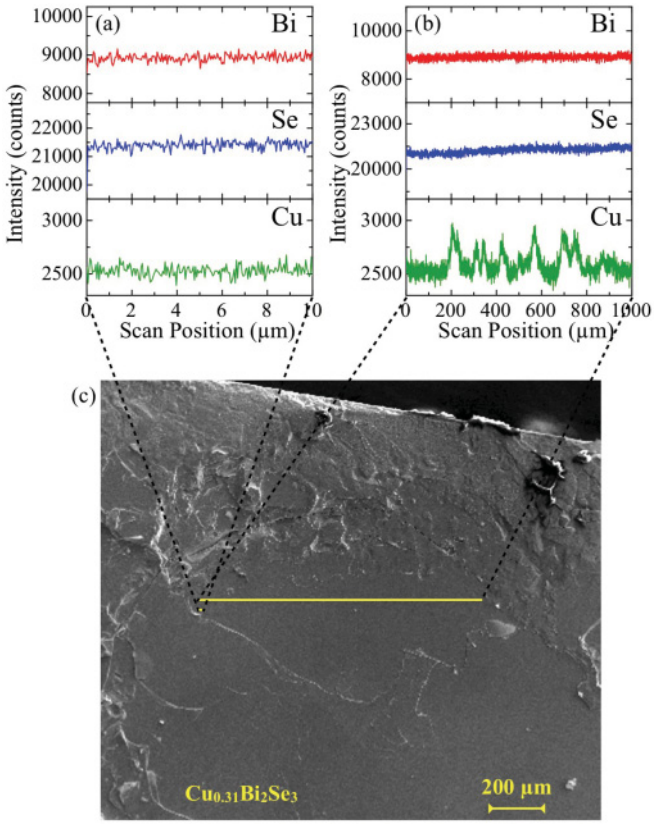

FIG. 2. (Color online) EPMA analyses of the cleaved surface of a sample with $x = 0.31$. Panels (a) and (b) summarize scans along two lines of 10 μm and 1 mm lengths, respectively, sketched in panel (c). One can see that the local Cu concentration is uniform on the μm scale, but it is inhomogeneous on the sub-mm scale.

the distributions of Bi and Se are essentially homogeneous on any length scale, as evidenced by the constant intensity of the respective characteristic x-ray. On the other hand, the distribution of Cu shows a variation of up to ~20% on the sub-mm length scale [Fig. 2(b)], although on the 10-μm length scale the Cu distribution is usually homogeneous [Fig. 2(a)]. Since the averaged Cu concentration of this sample determined from the mass change was 0.31, the spatial variation of ~20% corresponds to the variation in x of ~0.06.

III. SAMPLE CHARACTERIZATIONS

The superconducting samples were characterized by measuring the dc magnetization M and transport properties. To take the magnetization data, a commercial SQUID magnetometer (Quantum Design, MPMS) was used with the magnetic field applied parallel to the ab plane. The samples were cooled down in zero-magnetic field (zero-field cooled, ZFC) to the lowest accessible temperature $T = 1.8$ K; then a small dc field of $B = 0.2$ mT was applied and the magnetization was measured upon increasing temperature. After passing through T_c, defined as the onset of the drop in the $M(T)$ curves, data were again taken upon decreasing the temperature back to 1.8 K (field cooled, FC). The superconducting shielding fraction of a sample was estimated from its magnetic moment at $T = 1.8$ K after ZFC. The resistivity ρ_{xx} and the Hall coefficient R_H were measured by a standard six-probe technique, where the electrical current was applied in the ab plane.

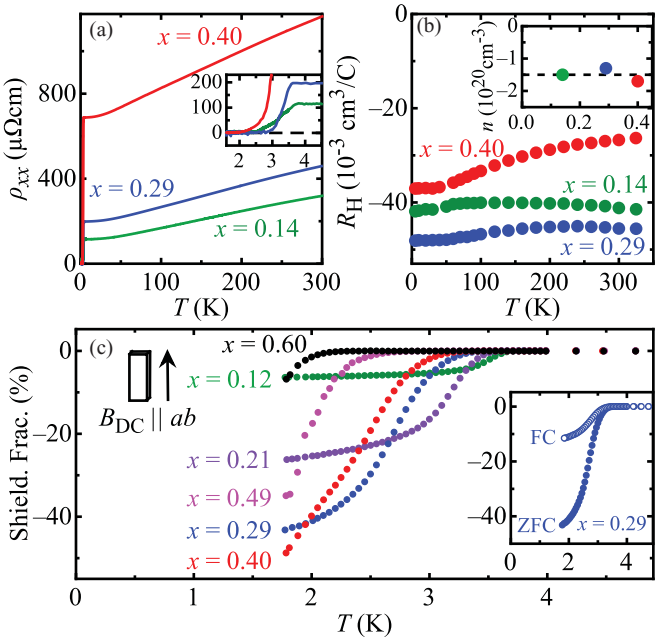

FIG. 3. (Color online) (a) Temperature-dependent resistivity of $Cu_xBi_2Se_3$ for $x = 0.14$, 0.29, and 0.40. The inset gives an enlargement around the superconducting transition. (b) Temperature dependence of the Hall coefficient R_H and the x-dependence of the charge-carrier concentration n (inset). (c) Temperature dependence of the superconducting shielding fraction in $B = 0.2$ mT after ZFC for various Cu concentrations $0.12 \leqslant x \leqslant 0.60$. For $x = 0.29$, the ZFC and FC data are exemplarily shown in the inset.

With our electrochemical intercalation technique, we have successfully synthesized samples which superconduct above 1.8 K for Cu concentrations of $0.09 \leqslant x \leqslant 0.64$. Figure 3(a) shows the resistivity data of $Cu_xBi_2Se_3$ for three selected Cu concentrations $x = 0.14, 0.29$, and 0.40 measured in zero field. All those samples exhibit a metallic temperature dependence above T_c and show zero resistance below T_c, see the expanded view in the inset of Fig. 3(a). With increasing Cu concentration, the absolute value of ρ_{xx} increases; especially, between $x = 0.29$ and 0.40, a strong rise in the absolute value is observed, which implies that a high Cu concentration enhances the disorder in the samples. Figure 3(b) summarizes the temperature dependences of R_H for the three samples, which are generally weak. The inset shows the x-dependence of the charge-carrier concentration n determined from the low-temperature value of R_H. It is striking that, despite the factor of three difference in the Cu concentration, the change in n is very small: $n = 1.5 \times 10^{20}$, 1.3×10^{20}, and 1.7×10^{20} cm^{-3} for $x = 0.14$, 0.29, and 0.40, respectively. Furthermore, those values correspond to only ~2% of electron doping. This is totally inconsistent with the expectation that there should be electron carriers with the nominal fraction of x in $Cu_xBi_2Se_3$. Therefore, there must be some side reaction taking place in $Cu_xBi_2Se_3$ to significantly reduce the actual electron carriers. In this regard, a similar problem was previously noted in a study of Cu intercalation into Bi_2Te_3, and it was proposed that Cu^+ reacts with the matrix to form a four-layer lamellar

structure Cu–Te–Bi–Te that annihilates electrons.[37] If a similar reaction occurs in $Cu_xBi_2Se_3$, it would be

$$Cu^+ + 2Bi_2Se_3 + e^- \rightarrow [CuBiSe_2][Bi_3Se_4^-] + h. \quad (3)$$

The formation of this type of structural defects can indeed explain the small n values observed in $Cu_xBi_2Se_3$.

Figure 3(c) summarizes the temperature dependences of the shielding fraction in samples with various x values. The onset temperatures of superconductivity in the magnetization data are slightly lower than the onset of the resistivity transition in respective samples, which is usual for disordered superconductors. The right inset of Fig. 3(c) shows the ZFC and FC data for $x = 0.29$, and other samples exhibited similar differences between the two. We note that samples with $x \geqslant 0.70$ were also prepared, but they did not show any superconducting transition above 1.8 K; however, it is possible that they exhibit superconductivity at lower temperatures.

IV. PHASE DIAGRAM AND DISCUSSIONS

Figure 4(a) shows the phase diagram of T_c vs x based on our measurements of more than 40 samples, and Fig. 4(b) summarizes the shielding fraction of those samples at 1.8 K. The lowest x value at which we found superconductivity was 0.09, where T_c was already 3.45 K; however, in spite of this relatively high T_c, the superconducting signal was very weak with a shielding fraction of only around 1%. For slightly larger x values around 0.12–0.15, the maximum values of T_c are found, but the shielding fractions were less than 20%, which is in agreement with the earlier report by Hor *et al.*[29] Intriguingly, T_c gradually decreases with increasing x down to $T_c \approx 2.2$ K for $x = 0.64$, which is the highest Cu concentration for which we could clearly confirm the superconductivity.

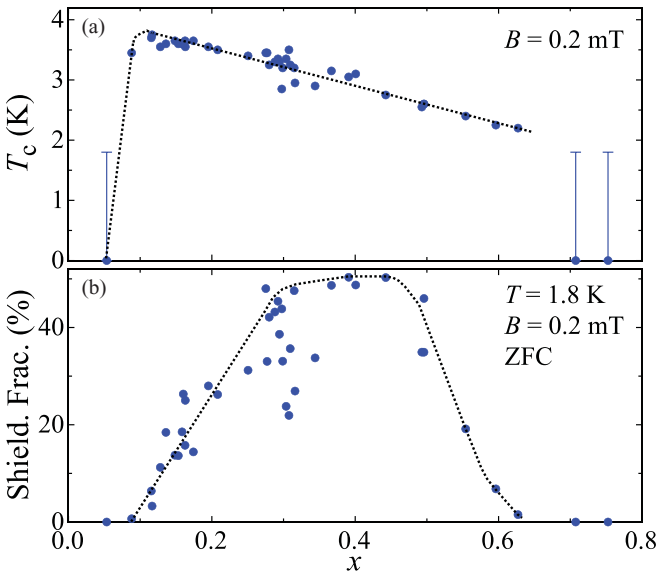

FIG. 4. (Color online) Cu concentration x dependence of (a) the critical temperature and (b) the shielding fraction at 1.8 K. These T_c data were extracted from the onset of superconductivity in magnetization measurements, the shielding-fraction data from the ZFC magnetization at $T = 1.8$ K, see Fig. 3(c).

Although T_c seems to be quite robust and reproducible, the shielding fraction exhibits a scattering among different samples even with similar x values, as can be seen in Fig. 4(b). Nevertheless, there is a clear trend that samples with maximal shielding fractions are obtained only for $0.3 \leqslant x \leqslant 0.5$ and the shielding fraction is reduced systematically (almost linearly) as x becomes smaller than $x \simeq 0.3$. This trend, together with the EPMA result that the actual Cu concentration varies on a sub-mm scale, suggests that $Cu_xBi_2Se_3$ has a tendency to phase segregate and that there is a spontaneous formation of small islands in which the local Cu concentration is essentially the optimum value for superconductivity. In view of the fact that the T_c of this material is uncharacteristically high for a low-carrier-density superconductor[38] with $n \sim 10^{20}$ cm^{-3}, the present observation seems to imply that the inhomogeneous nature of the superconductivity may partly be responsible for the anomalously high T_c.[39] Furthermore, the unexpected drop of the shielding fraction for $x > 0.5$ suggests that the inhomogeneity may be necessary for the occurrence of superconductivity in this material.

If $Cu_xBi_2Se_3$ indeed has a tendency toward phase segregation to spontaneously form small superconducting islands, it naturally explains why a high-temperature annealing is necessary for activating the superconductivity: It allows Cu atoms to move and promotes the formation of superconducting islands. If annealed at too high a temperature, the material seems to melt partly, the crystal structure degrades, and eventually the superconductivity is destroyed irreversibly. Indeed, the melting temperature of $Cu_xBi_2Se_3$ appears to be systematically reduced with x, and our test sample with $x = 1.4$, which was initially rectangular shaped, became sphere-like after annealed at 560 °C. (Note that the melting point of pure Bi_2Se_3 is 706 °C.) Therefore, the optimal annealing temperature corresponds to the one that maximally promotes the motion of Cu atoms while avoiding degradation of the matrix due to partial melting.

V. SUMMARY

In summary, we have synthesized superconducting $Cu_xBi_2Se_3$ by an electrochemical intercalation method, which yields samples with much higher superconducting shielding fractions compared to those prepared by the melt-growth technique previously employed. The superconductivity was observed for $0.09 \leqslant x \leqslant 0.64$, which is much wider than previously reported, and the transition temperature T_c was found to show an unexpected monotonic decrease with x. Also, the largest attainable shielding fraction was found to be strongly dependent on x, and its x dependence suggests that $Cu_xBi_2Se_3$ has a tendency to phase segregate and form small superconducting islands.

ACKNOWLEDGMENTS

We acknowledge the technical support from the Comprehensive Analysis Center, Institute of Scientific and Industrial Research, Osaka University, for the ICP-AES and the EPMA analyses. This work was supported by JSPS (NEXT Program), MEXT (Innovative Area "Topological Quantum Phenomena" KAKENHI 22103004), and AFOSR (AOARD 10-4103).

*mkriener@sanken.osaka-u.ac.jp
†Corresponding author: y_ando@sanken.osaka-u.ac.jp

[1] L. Fu, C. L. Kane, and E. J. Mele, Phys. Rev. Lett. **98**, 106803 (2007).
[2] J. E. Moore and L. Balents, Phys. Rev. B **75**, 121306(R) (2007).
[3] R. Roy, Phys. Rev. B **79**, 195322 (2009).
[4] M. Z. Hasan and C. L. Kane, Rev. Mod. Phys. **82**, 3045 (2010).
[5] J. E. Moore, Nature **464**, 194 (2010).
[6] X. Qi and S. Zhang, Topological insulators and superconductors, e-print arXiv:1008.2026v1 (to be published).
[7] L. Fu and C. L. Kane, Phys. Rev. B **76**, 045302 (2007).
[8] H.-J. Zhang, C.-X. Liu, X.-L. Qi, X. Dai, Z. Fang, and S.-C. Zhang, Nat. Phys. **5**, 438 (2009).
[9] D. Hsieh, D. Qian, L. Wray, Y. Xia, Y. S. Hor, R. J. Cava, and M. Z. Hasan, Nature **452**, 970 (2008).
[10] A. A. Taskin and Y. Ando, Phys. Rev. B **80**, 085303 (2009).
[11] A. Nishide, A. A. Taskin, Y. Takeichi, T. Okuda, A. Kakizaki, T. Hirahara, K. Nakatsuji, F. Komori, Y. Ando, and I. Matsuda, Phys. Rev. B. **81**, 041309(R) (2010).
[12] Y. L. Chen, J. G. Analytis, J.-H. Chu, Z. K. Liu, S.-K. Mo, X. L. Qi, H. J. Zhang, D. H. Lu, X. Dai, Z. Fang, S. C. Zhang, I. R. Fisher, Z. Hussain, and Z.-X. Shen, Science **325**, 178 (2009).
[13] D. Hsieh, Y. Xia, D. Qian, L. Wray, F. Meier, J. H. Dil, J. Osterwalder, L. Patthey, A. V. Fedorov, H. Lin, A. Bansil, D. Grauer, Y. S. Hor, R. J. Cava, and M. Z. Hasan, Phys. Rev. Lett. **103**, 146401 (2009).
[14] Y. Xia, D. Qian, D. Hsieh, L. Wray, A. Pal, H. Lin, A. Bansil, D. Grauer, Y. S. Hor, R. J. Cava, and M. Z. Hasan, Nat. Phys. **5**, 398 (2009).
[15] T. Sato, K. Segawa, H. Guo, K. Sugawara, S. Souma, T. Takahashi, and Y. Ando, Phys. Rev. Lett. **105**, 136802 (2010).
[16] K. Kuroda, M. Ye, A. Kimura, S. V. Eremeev, E. E. Krasovskii, E. V. Chulkov, Y. Ueda, K. Miyamoto, T. Okuda, K. Shimada, H. Namatame, and M. Taniguchi, Phys. Rev. Lett. **105**, 146801 (2010).
[17] Y. L. Chen, Z. K. Liu, J. G. Analytis, J.-H. Chu, H. J. Zhang, B. H. Yan, S.-K. Mo, R. G. Moore, D. H. Lu, I. R. Fisher, S.-C. Zhang, Z. Hussain, and Z.-X. Shen, Phys. Rev. Lett. **105**, 266401 (2010).
[18] Z. Ren, A. A. Taskin, S. Sasaki, K. Segawa, and Y. Ando, Phys. Rev. B **82**, 241306(R) (2010).
[19] S. Xu, L. Wray, Y. Xia, R. Shankar, A. Petersen, A. Fedorov, H. Lin, A. Bansil, Y. Hor, D. Grauer, R. Cava, and M. Hasan, Discovery of several large families of Topological Insulator classes with backscattering-suppressed spin-polarized single-Dirac-cone on the surface, e-print arXiv:1007.5111v1.
[20] J. Xiong, A. C. Petersen, Dongxia Qu, R. J. Cava, and N. P. Ong, Quantum oscillations in a topological insulator Bi_2Te_2Se with large bulk resistivity, e-print arXiv:1101.1315.
[21] A. A. Taskin, Z. Ren, S. Sasaki, K. Segawa, and Y. Ando, Phys. Rev. Lett. **107**, 016801 (2011).
[22] L. Fu and C. L. Kane, Phys. Rev. Lett. **100**, 096407 (2008).
[23] A. P. Schnyder, S. Ryu, A. Furusaki, and A. W. W. Ludwig, Phys. Rev. B **78**, 195125 (2008).
[24] X.-L. Qi, T. L. Hughes, S. Raghu, and S.-C. Zhang, Phys. Rev. Lett. **102**, 187001 (2009).
[25] X.-L. Qi, T. L. Hughes, and S.-C. Zhang, Phys. Rev. B **81**, 134508 (2010).
[26] J. Linder, Y. Tanaka, T. Yokoyama, A. Sudbø, and N. Nagaosa, Phys. Rev. Lett. **104**, 067001 (2010).
[27] M. Sato, Phys. Rev. B **81**, 220504(R) (2010).
[28] L. Fu and E. Berg, Phys. Rev. Lett. **105**, 097001 (2010).
[29] Y. S. Hor, A. J. Williams, J. G. Checkelsky, P. Roushan, J. Seo, Q. Xu, H. W. Zandbergen, A. Yazdani, N. P. Ong, and R. J. Cava, Phys. Rev. Lett. **104**, 057001 (2010).
[30] L. A. Wray, S.-Y. Xu, Y. Xia, Y. S. Hor, D. Qian, A. V. Fedorov, H. Lin, A. Bansil, R. J. Cava, and M. Z. Hasan, Nat. Phys. **6**, 855 (2010).
[31] M. Kriener, K. Segawa, Z. Ren, S. Sasaki, and Y. Ando, Phys. Rev. Lett. **106**, 127004 (2011).
[32] L. P. Caywood and G. R. Miller, Phys. Rev. B **2**, 3209 (1970).
[33] A. Vaško, L. Tichý, J. Horák, and J. Weissenstein, Appl. Phys. **5**, 217 (1974).
[34] For example, the wavelength dispersive X-ray spectroscopy (WDS) analysis, which is a non-destructive method and is often employed in the chemical content analysis, is sensitive to relative differences, but it is not good at giving absolute numbers.
[35] As for the optimization of the annealing time, we have annealed several samples that were already annealed at 560 °C for 2 h for various additional durations of time at the same temperature; annealing for a few additional hours did not improve the shielding fraction, and a long-term annealing (more than a day) usually resulted in a decrease in the shielding fraction. Separately, we found that an annealing for less than 1 h did not establish superconductivity. We therefore settled on the 2-h annealing procedure to minimize the sample preparation time.
[36] The detailed results of the ICP-AES analyses are the following: the x values of the eight samples determined from the mass change were 0.117, 0.128, 0.266, 0.286, 0.293, 0.295, 0.308, and 0.318; for these samples, the x values determined by the ICP-AES analyses were 0.114, 0.128, 0.279, 0.300, 0.299, 0.282, 0.303, and 0.319, respectively; therefore, the differences between the two were 0.003, 0.000, −0.013, −0.014, −0.006, 0.013, 0.005, and −0.001.
[37] J. Bludská, S. Karamazov, J. Navrátil, I. Jakubec, and J. Horák, Solid State Ionics **171**, 251 (2004).
[38] M. L. Cohen, in *Superconductivity*, edited by R. D. Parks (Marcel Dekker, New York, 1969), Vol. 1, chap. 12.
[39] I. Martin, D. Podolsky, and S. A. Kivelson, Phys. Rev. B **72**, 060502(R) (2005).